AUT Journal of Electrical Engineering

AUT J. Elec. Eng., 52(2) (2020) 169-178
DOI: 10.22060/eej.2020.18045.5342

Hybrid Fuzzy Algorithm for the Novel Yokeless Axial Flux-Switching Permanent-Magnet Motor

H. Radmanesh[1], J. Rahmani Fard[2,*]

[1]Faculty of Electrical Engineering, Shahid Sattari Aeronautical University of Science and Technology, Tehran, Iran.
[2]Department of Power Engineering, Faculty of Electrical Engineering, Pooyesh institute of higher education, Qom, Iran

ABSTRACT: -A new fuzzy PI control algorithm for a novel yokeless and segmented armature axial flux-switching sandwiched permanent-magnet motor (YASA-AFFSSPM) is proposed in this paper. In the conventional fuzzy PI control of the permanent magnet synchronous motor the torque ripple is large and the control accuracy is not high precise. A new fuzzy PI control algorithm is proposed to solve this problem, and a prototype of the YASA-AFFSSPM motor is fabricated and the method is tested. The simulation and experimental results demonstrate that the new fuzzy PI controller can improve the robustness of the system and improve the precision. Further, the dynamic performance of the YASA-AFFSSPM motor is excellent.

Review History:

Received: 2020-03-04
Revised: 2020-06-09
Accepted: 2020-07-22
Available Online: 2020-12-01

Keywords:

flux-switching permanent-magnet motor
MRAS adaptive system
fuzzy PI control

Introduction

The future of road transport is electric; the pure electric vehicles (EVs) will occupy our roads within the foreseeable future [1]. Vehicles equipped with the traditional internal combustion engines (ICE) have existed for over a hundred years [2]. Although ICE vehicles have been improved by modern automotive electronics technology, only low efficiency is offered. One of the most promising technologies is electric vehicles which can lead to significant developments in energy utilization efficiency, vehicle performance, and emission reductions [3]. Awareness of environmental problems is growing dramatically throughout the world. This is leading to a tremendous interest in developing non-polluting electric vehicles. The EV uses at least one electric motors or traction motors for propulsion. Through a collector system an EV might be controlled by electricity from off-vehicle sources, or might act naturally contained with an electric generator, solar panel and battery to change over fuel to electricity [4]. Electric vehicles (EV) are accomplishing lower automobile discharges. EV motors need high speed and torque characteristics to cover the whole vehicle working range and furthermore cause high proficiency for best distance [5]. It is particularly important to expand engine effectiveness in the low torque region, since it usually used in urban driving and fuel economy measurement.

In recent years, because of the improved awareness of environmental protection and the progressive exhaustion of fossil fuels, the EVs have gotten more consideration. In a power system configuration, increments in fuel prices and environmental concerns have led to adjustments [6]. One of the critical changes is expanding utilization of new energy resources like high power batteries, high-capacity, EVs and renewable energy resources in a power grid. Many experts have noticed that these new energy resources can conquer environmental issues and fuel price [7]. To improve the energy efficiency and renewable energy penetration, the EVs can be conveyed with low cost [8]. PM motors are becoming increasingly attractive with the approach of high-energy-permanent magnet materials. The permanent magnet machines are much more perfect with solar power applications [9]. Electrical machines (both motors and generators) are a constantly developing and significant application for permanent magnets [10].

Flux switching permanent magnet synchronous motor (FMSM) has the characteristics such as large output torque, fast speed response and high reliability, so it can be widely used in high-performance and high precision control.

In the permanent magnet synchronous motor control system, the speed loop usually adopts the PI control algorithm. Although the PI control algorithm is relatively simple, there is a problem of adjusting the PI parameters, so the traditional PI also has limitations. The fuzzy control algorithm [14] has been applied to the permanent magnet synchronous control system. The fuzzy controller is different from the traditional

*Corresponding author's email: javad.rahmani.fard@gmail.com

PI control. It does not depend on the accurate mathematical model of the controlled object, and is not easily affected by the ideal nonlinear controller [13].

However, the fuzzy controllers also have a big disadvantage. When the motor load suddenly increases, the fuzzy PI control has many difficulties to effectively eliminate the system steady-state error, so the control precision is not high, which is mainly due to the lack of integral effect controller.

Moreover, due to its specific features, the fuzzy controller can easily ruin the performance of the control system, which is difficult to achieve with the desired control accuracy. Therefore, to improve the steady-state performance of FSPM control system, by analyzing the principle of the basic fuzzy controller, the traditional method is more improved, and the integration of the error signal is added.

The sensor-less research is mainly divided into low speed and medium speed. In low speed, high frequency injection method is generally used, but this method is used for motors with a salient pole, and the use of this method is limited. In the case of medium and high-speed, the sensor-less control method includes the model reference adaptation method [16-17], Extended Kalman Filter method and sliding mode variable structure method.

The Extended Kalman Filter method has a large amount of computation, and the sliding mode control algorithm has the problem of sliding mode. In comparison, the model reference adaptation method has good stability and simple parameter identification [19-21], which is not affected by the system control method.

In [22] a novel yokeless and segmented armature axial flux-switching sandwiched permanent-magnet motor (YASAAFFSSPM) is proposed which has good fault tolerant capability. In this paper a new fuzzy PI control algorithm for a 12 slots/19poles YASA-AFFSSPM motor is proposed.

1. ConFiguration the YASA-AFFSSPM Motor

Fig.. 1 shows the configuration of the YASA-AFFSSPM with 12 stator slots (S) and 19 rotor poles (P). In this configuration, there is not stator yoke; also two rotors are axially unaligned. Moreover, a special concentrated-coil winding, that has a displacement winding factor equal to 1, is used [22].

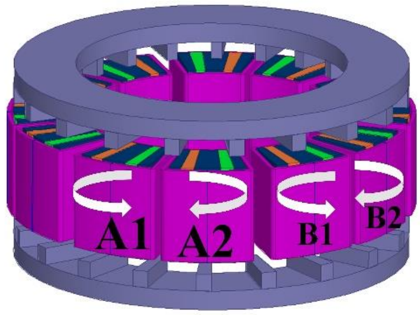

Fig. 1: Configuration of the YASA-AFFSSPM motor.

2. Model Reference Adaptive Systems Algorithm

Model Reference Adaptive Systems (MRAS) is a control algorithm in the case of the systems with uncertain variables.

The main idea of MRAS is to use the equations with the parameters to estimate the adjustable model of the system. The equations without the unknown parameter are as the reference model of the system, and the adjustable model and the reference model have the same output in physical meaning.

Taking the output of the reference model as the ideal response, and then through the adaptive mechanism, the parameters of the adjustable model of the system are adjusted in real time, so that the difference between the output of the reference model and the adjustable model is zero. Thus, the output of the control system can be well tracked by the output of the reference model. The schematic diagram of the MRAS principle is shown in Fig. 2. As can be seen from Fig. 2, x, the output value of the reference model, is the ideal system dynamic response. The reference model output is used as a given performance parameter, and the given parameters performance are compared with the measured parameters performance. When the controlled object deviates from the optimal trajectory due to changes in the external environment or working conditions, the error can be obtained by subtracting the reference model output, x, and adjustable model output, $\hat{x}$. The obtained error ε enters the adaptive mechanism. Then, the feedback of the adjustable model is adjusted to make the output of the adjustable model. $\hat{x}$ is consistent with the x of the reference model, which causes the ε becomes zero.

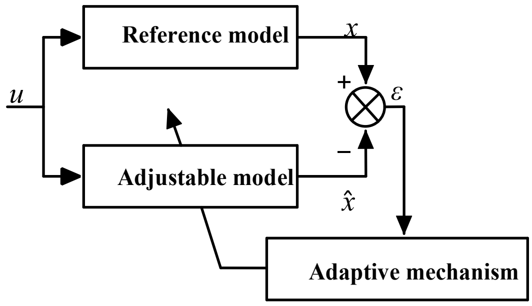

Fig. 2: The schematic of the MRAS.

3. Mathematical Model of YASA-AFFSSPM Motor

The MRAS algorithm uses the actual operating state of the motor as a reference model. The motor speed and current, which are estimated, are used as an adjustable model. In this paper, current values are selected as the reference values of the reference model and the adjustable model. The difference between actual current and estimated current is given through the adaptive mechanism to the adjustable model. The estimated value tracks the actual value so that the motor runs stably. In the synchronous rotation d-q coordinate system, the voltage equations of the YASA-AFFSSPM are as follows

$$u_d = R_s i_d + L_s p i_d - \omega_r L_s i_q \tag{1}$$

$$u_q = R_s i_q + L_s p i_q - \omega_r L_s i_d + \omega_r \psi_f \tag{2}$$

Where u_d and u_q are the axes stator voltages, $i_d$and i_q are the $dq-$ axes stator currents, ψ_f is the rotor permanent magnet flux linkage, ω_r is the electrical angular velocity and R_s is the armature winding resistance. The simplification (1) and (2) gives (3) and (4) which are used as reference model.

$$pi_d + \frac{p\psi_f}{L_s} = -\frac{R_s}{L_s}\left(i_d + \frac{\psi_f}{L_s}\right) + \omega_r i_q + \frac{1}{L_s}\left(u_d + R_s\frac{\psi_f}{L_s}\right). \tag{3}$$

$$pi_q = -\omega_r\left(i_d + \frac{\psi_f}{L_s}\right) - \frac{R_s}{L_s}i_q + \frac{1}{L_s}u_q. \tag{4}$$

By definition $i'_d = i_d + \frac{\psi_f}{L_s}$, $i'_q = i_q$, $u'_d = u_d + R_s\frac{\psi_f}{L_s}$, $u'_q = u_q$, the reference model is as follows:

$$pi'_d = -\frac{R_s}{L_s}i'_d + \omega_r i'_q + \frac{1}{L_s}u'_d. \tag{5}$$

$$pi'_q = -\omega_r i'_d - \frac{R_s}{L_s}i'_q + \frac{1}{L_s}u'_q. \tag{6}$$

where and u'_q are the $dq-$axes stator reference model voltages, i'_d and i'_q are the $dq-$ axes stator reference model currents. The adjustable model is constructed by (5) and (6) as

$$p\tilde{i}'_d = -\frac{R_s}{L_s}\tilde{i}'_d + \widetilde{\omega_r}\tilde{i}'_q + \frac{1}{L_s}u'_d. \tag{7}$$

$$p\tilde{i}'_q = -\widetilde{\omega_r}\tilde{i}'_d - \frac{R_s}{L_s}\tilde{i}'_q + \frac{1}{L_s}u'_q. \tag{8}$$

where $\tilde{i}'_d$ and $\tilde{i}'_q$ are the dq-axes stator adjustable model currents, $\tilde{\omega}_r$ is estimated electrical angular velocity. The error $\varepsilon = i'_s - \tilde{i}'_s$ can be obtained by (5) — (7) and (6) — (8).

$$p\varepsilon_d = -\frac{R_s}{L_s}\varepsilon_d + \omega_r\varepsilon_q + (\omega_r - \widetilde{\omega_r})p\tilde{i}'_q. \tag{9}$$

$$p\varepsilon_q = -\frac{R_s}{L_s}\varepsilon_q - \omega_r\varepsilon_d - (\omega_r - \widetilde{\omega_r})p\tilde{i}'_d. \tag{10}$$

where $\varepsilon = i'_d - \tilde{i}'_d$ and $\varepsilon = i'_q - \tilde{i}'_q$. The parameters in MRAS usually use a proportional integral structure. From the (9)-(10) and Popov hyperstability theory, we can write

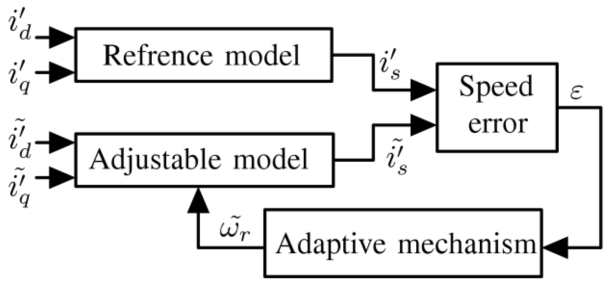

Fig. 3: The law of MRAS adaptive system.

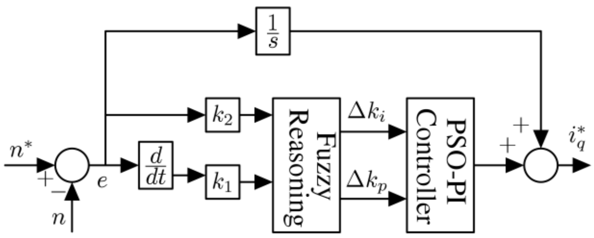

Fig. 4: Hybrid fuzzy control schematic.

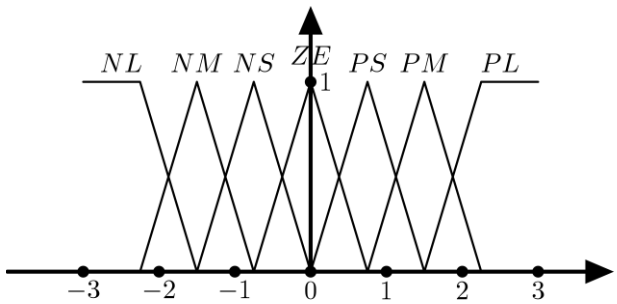

Fig. 5: System input deviation and membership function of .

$$\widetilde{\omega_r} = \int_0^t k_i\left(i'_d\tilde{i}'_q - \tilde{i}'_d i'_q\right)d\tau + k_p\left(i'_d\tilde{i}'_q - \tilde{i}'_d i'_q\right) + \widetilde{\omega_r}(0) \tag{11}$$

The term $i'_d\tilde{i}'_q - i'_q\tilde{i}'_d$ generates electrical angular velocity estimation $\tilde{\omega}_r$ through PI regulator and $\tilde{\omega}_r$makes adjustable model value $\tilde{i}'_s$, which tends to reference model value i'_s. Therefore, stator current error tends to zero, and $\tilde{\omega}_r$ gradually approaches the actual speed and making system run stable, as shown in Fig. 3.

According to $i'_d = i_d + \frac{\psi_f}{L_s}$, $i'_q = i_q$, (11) is written as

$$\widetilde{\omega_r} = \int_0^t k_i\left(i_d\tilde{i}_q - \tilde{i}_d i_q - \frac{\psi_f}{L_s}(i_q - \tilde{i}_q)\right)d\tau + k_p\left(i_d\tilde{i}_q - \tilde{i}_d i_q - \frac{\psi_f}{L_s}(i_q - \tilde{i}_q)\right) + \widetilde{\omega_r}(0). \tag{12}$$

TABLE 1. FUZZY CONTROL RULE TABLE

de \ e	NL	NM	NS	ZE	PS	PM	PL
NL	NL	NL	NL	NM	NM	NS	ZE
NM	NL	NL	NM	NM	NS	ZE	PS
NS	NL	NM	NM	NS	ZE	PS	PM
ZE	NM	NM	NS	ZE	PS	PM	PM
PS	NM	NS	ZE	PS	PM	PM	PL
PM	NS	ZE	PS	PM	PM	PL	PL
PL	ZE	PS	PM	PM	PL	PL	PL

4. Optimized design of the fuzzy PI regulator

Fuzzy control is the fuzzy set theory, which expresses the experience of human experts in an algorithmic language that can be recognized by computers, therefore, human intelligence is simulated and the control effect required by the system is provided. The derivative of the speed deviation and the speed deviation are used as the input of the fuzzy controller, as shown in Fig.. 4.

As seen in Fig. 4, the speed deviation e is the difference between the speed reference value n^* and the estimated feedback value n ie $e = n^* - n$. The deviation e passes through the gain k_1 and the rate of changes of the e through the gain k_2. These are as fuzzy reasoning inputs. Fig. 5 shows the membership function of the system input deviation e and the deviation change rate $\frac{de}{dt}$. The fuzzy inference rules are shown in Table 1.

PSO is a meta-heuristic algorithm applied to solve continuous multi-objective optimization problems. Therefore, the PSO approach is applied to the controller, and the basic principle is represented by (13)

$$\begin{cases} K^t = \left(K_P^t, K_I^t\right) \\ V_{j,g}^{(t+1)} = \omega V_{j,g}^{(t)} + c_1\left(p_{best} - K_{j,g}^{(t)}\right) rand() \\ \qquad + c_2\left(g_{best} - K_{j,g}^{(t)}\right) rand() \\ K_{j,g}^{(t+1)} = K_{j,g}^{(t)} + V_{j,g}^{(t-1)} \end{cases} \tag{13}$$

where c_1, c_2 are the learning constants, ω is the inertia weight, V is the velocity of the particle, t is the pointer of iterations, $rand$ ()is the normalized random number $\in$ [0,1], p_{best} is the best previous position of the swarm, g_{best} is the best position attained among all the agents of the swarm, K_P and K_I are the proportional and integral gain, respectively. The flowchart in Fig. 6 explains the process of PSO-PI concisely.

The diagram of the YASA-AFFSSPM control system with hybrid Fuzzy controller is shown in Fig. 7.

As seen from Fig..7, the system is a double closed loop vector control system consisted of a speed loop as an outer loop and a current loop as an inner loop.

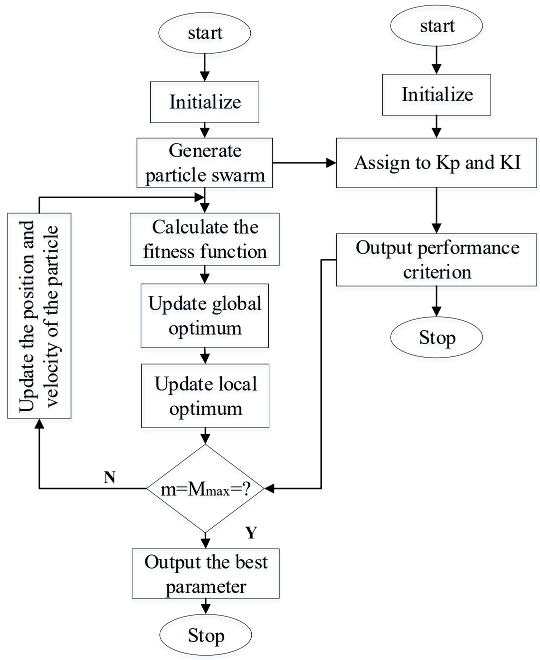

Fig. 6. Flowchart of the proposed control strategy in the PSO-PI scheme

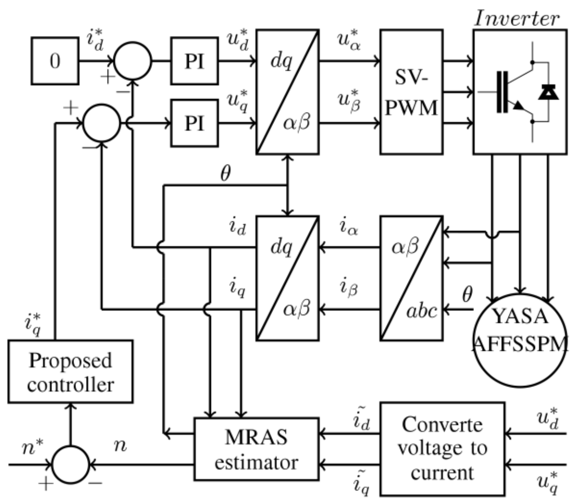

Fig.. 7: The diagram of the YASA-AFFSSPM control system with hybrid Fuzzy controller.

TABLE 2. PARAMETERS OF THE INVESTIGATED MOTOR

Item	value
Rated speed (rpm)	200
Rated torque $(N.m)$	12
Rated power(kW)	0.75
Stator inductance (mH)	5
PM flux linkage (Wb)	0.10
Stator resistance (Ω)	0.65
dq axes rated current$I_d = I_q/(A)$	10
Sampling time(s)	10^{-4}

The motor speed and rotation angle are obtained by MRAS

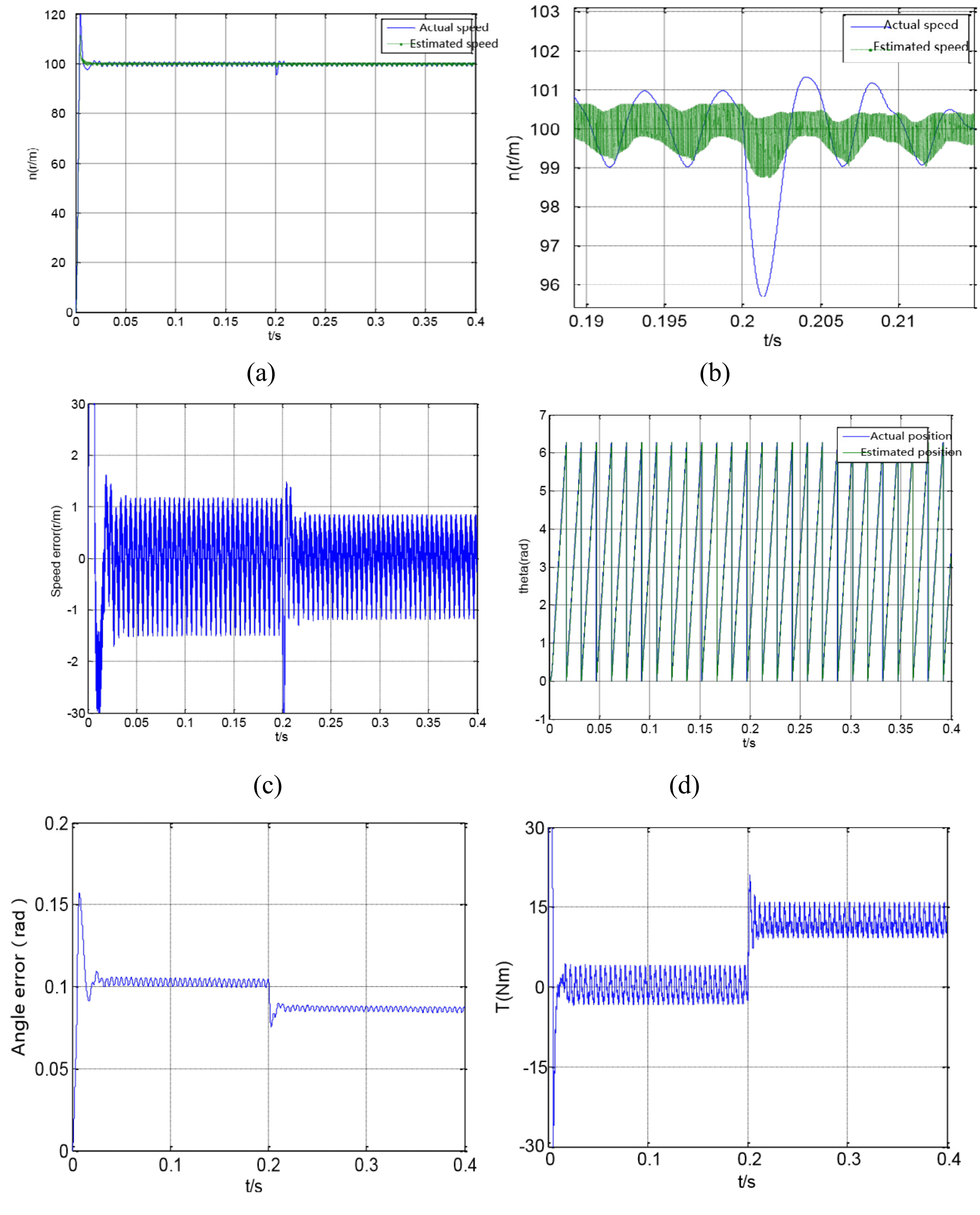

Fig. 8. Traditional fuzzy PI control simulation waveforms. (a) Speed waveform (b) Speed magnified waveform (c) Speed error waveform (d) Angle waveform (e) Angle error waveform (f) Torque waveform.

estimation. The speed is compared with the given speed. The difference is the input to the hybrid fuzzy controller and the $\frac{1}{s}$ is added to hybrid fuzzy controller. The output of the hybrid fuzzy controller is i_q^*.

By using the estimated rotation angle as the reference angle of the coordinate rotation transformation, the voltage in the $\alpha\beta$coordinate system is obtained, also, the PWM switching signal is generated by SVPWM modulation, and the inverter is controlled to control the YASA-AFFSSPM motor.

5. Simulation results

The control technology proposed in this paper is analyzed by simulation results in this section. The main parameters of the investigated motor are shown in Table 2.

In traditional fuzzy PI control, the simulation waveforms are shown in Fig. 8. Moreover, with the new fuzzy PI control, the simulated waveforms are shown in Fig. 9.

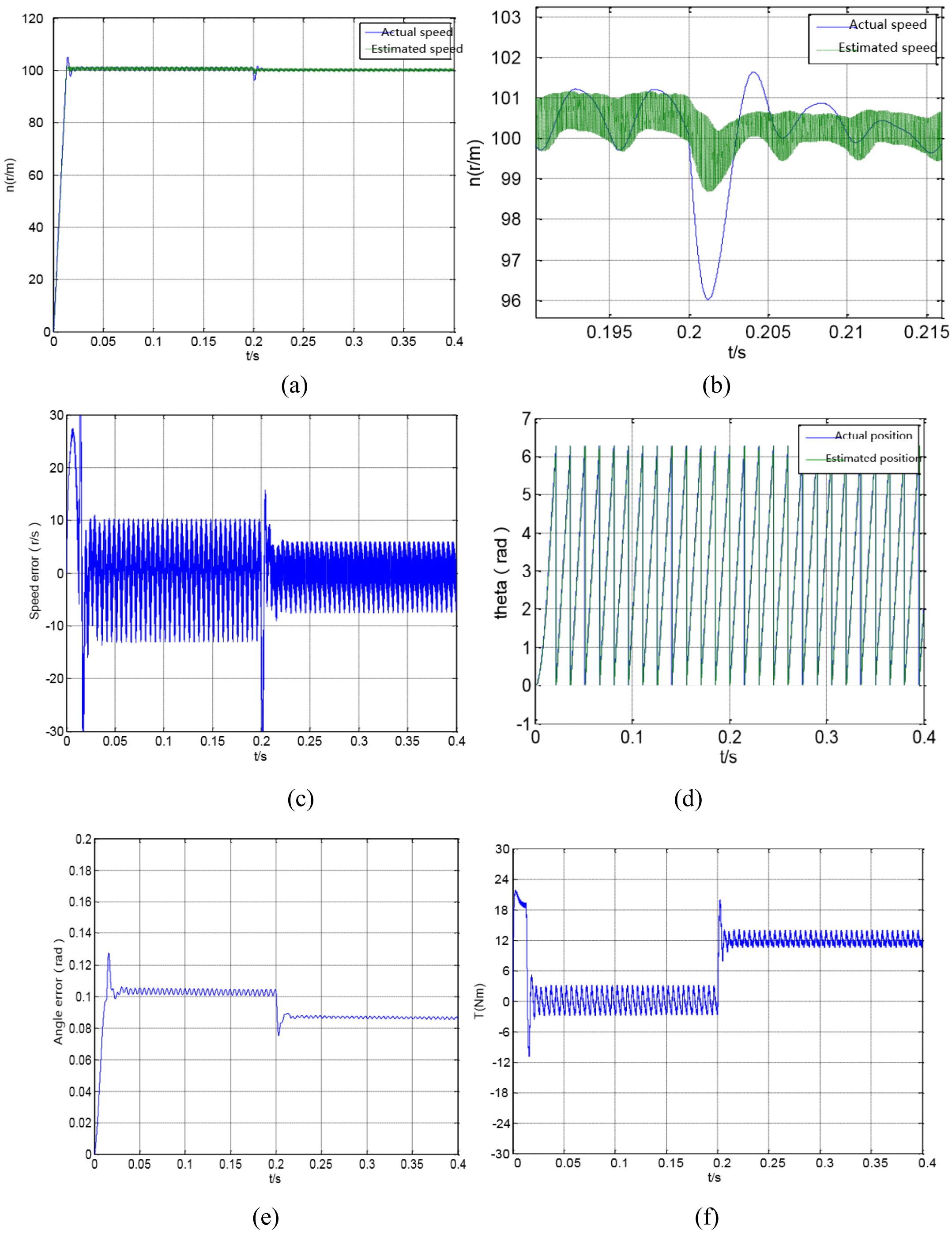

Fig. 9. Simulation waveform of new fuzzy PI control. (a) Speed waveform (b) Speed magnified waveform (c) Speed error waveform (d) Angle waveform (e) Angle error waveform (f) Torque waveform.

By comparing the simulation waveforms in (a) and (b) in Fig. 8 with (a) and (b) in Fig. 9, it can be concluded, when using traditional fuzzy PI control, the ratio of overshoot is greater than that of the new fuzzy PI control, and has many vibrations. Moreover, the speed is stable at 0.215s, while in the new fuzzy PI control, the speed is almost stable at 0.200s. By comparing the simulation waveforms in (c) Fig. 8 with (c) in Fig. 9, it can be concluded that the speed error of the new fuzzy PI control is almost stable between -7 and 7. Moreover, the speed error of the traditional fuzzy PI control eventually stabilizes between -11 and 9. So the speed error of the new fuzzy PI control is smaller than that of the traditional fuzzy PI control. By comparing the simulation waveforms in (a) and (b) in Fig. 8 with (a) and (b) in Fig. 9, it can be concluded that the angle error of the new fuzzy PI control is more stable than the traditional fuzzy PI control. A comparison between the simulation waveforms in (f) in Fig. 8 and (f) in Fig. 9 shows that the torque ripple of the new fuzzy PI control is smaller than the torque ripple of the traditional fuzzy PI control. For better comparison, the results are listed in table 3.

TABLE 3. COMPARISON BETWEEN TWO FUZZY PI CONTROL

Items	Traditional fuzzy PI control	new fuzzy PI control
the ratio of overshoot	20%	7%
settling time	0.215s	0.200s
speed error	between -11 and 9	between -7 and 7
torque ripple	37%	18%

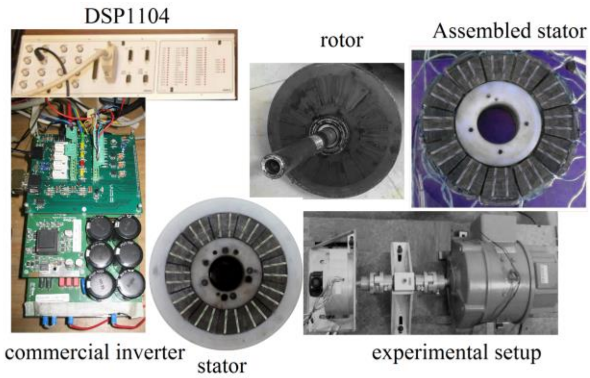

Fig. 10: Prototype machine and the experimental setup.

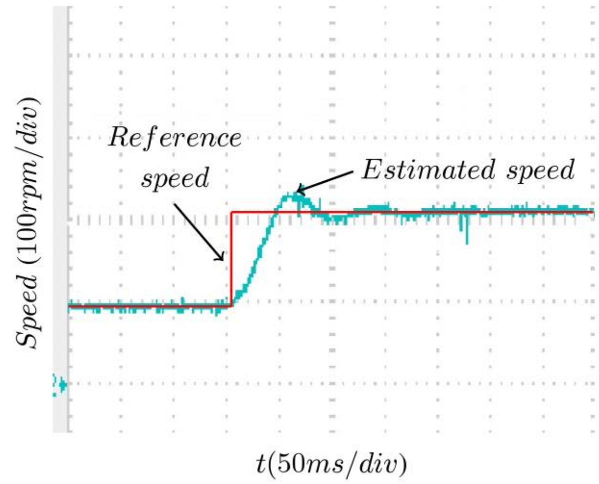

Fig.. 11. Estimated Speed in conventional fuzzy-PI controller.

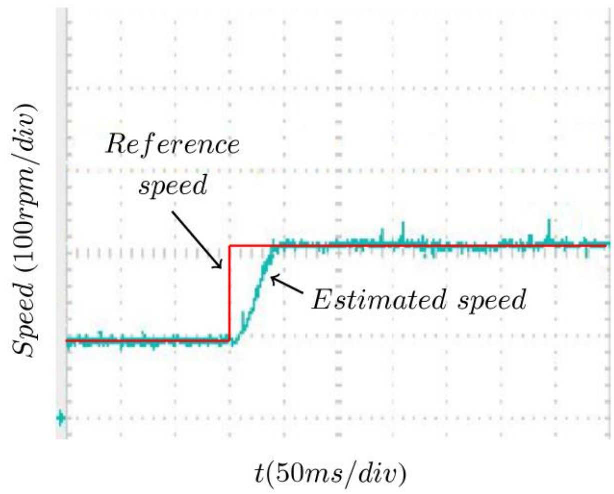

Fig. 12: Estimated Speed in proposed fuzzy-PI controller.

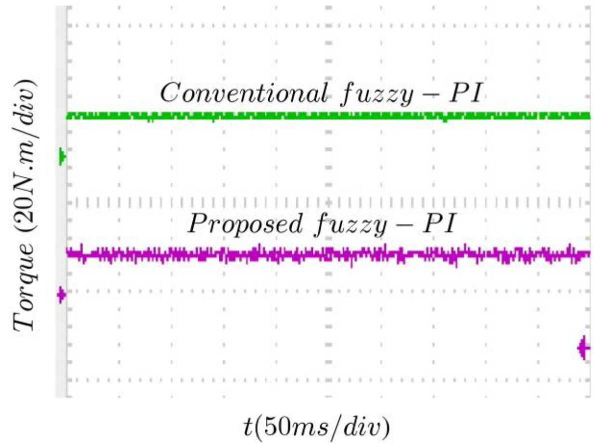

Fig. 13: Torque waveform.

6. Experimental results

Fig. 10 depicts the prototype of the 12S/19P YASA-AFFSSPM machine and the experimental setup. The DSP1104 is the core of the digital control system. The emulate load is a 1.5 hp separately excited DC machine. At first, the load torque is 8 N.m. In the conventional and proposed fuzzy-PI control, the experimental results are shown in this section.

A. Performance during speed changes

The reference speed suddenly changes from 100rpm to 200rpm, but the load torque is constant. As seen in Fig..11 and 12, in conventional fuzzy-PI controller, the speed will be stable in about 140ms while it will be stable in about 100ms in proposed fuzzy-PI controller.

Moreover, a comparison of the Fig.11 ~ Fig.12 shows that the overshoot ratio and torque ripple in the new fuzzy-PI controller are smaller than those of in the conventional fuzzy-PI controller. As seen from Fig. 14 that the estimated position and actual position.

B. Performance during torque changing

In order to investigate the dynamic response performance of the proposed method, the torque suddenly is increased. The initial value of the torque reference is 8 N.m, the sudden change of the load torque occurs, which is 12 N.m. The results of q-axis current response and torque response are shown in Fig.s. 15 and 16.

7. Conclusion

This paper designs a model reference adaptive control system for a new fuzzy algorithm. The conventional fuzzy-

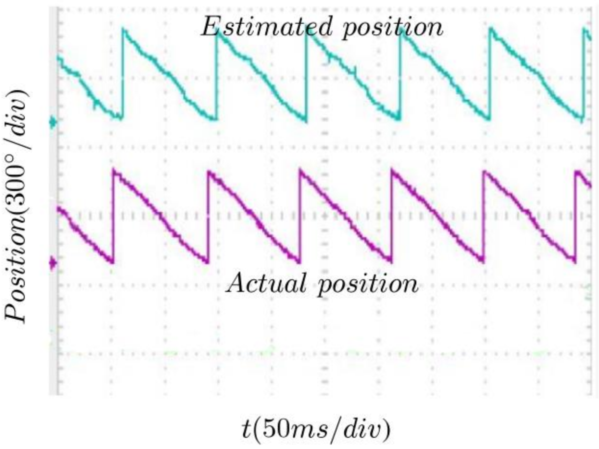

Fig. 14: Position waveform.

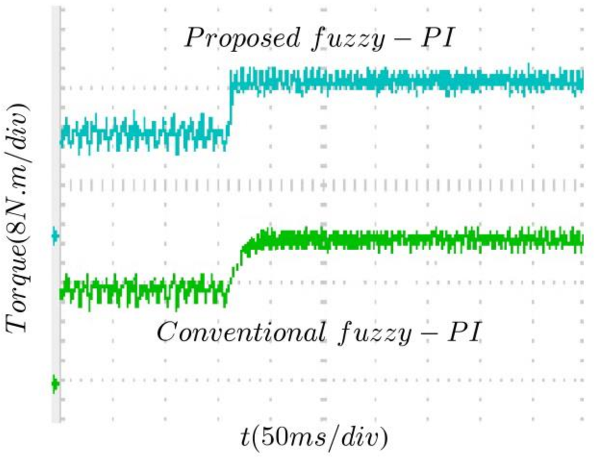

Fig. 15: Troque during suddenly changes.

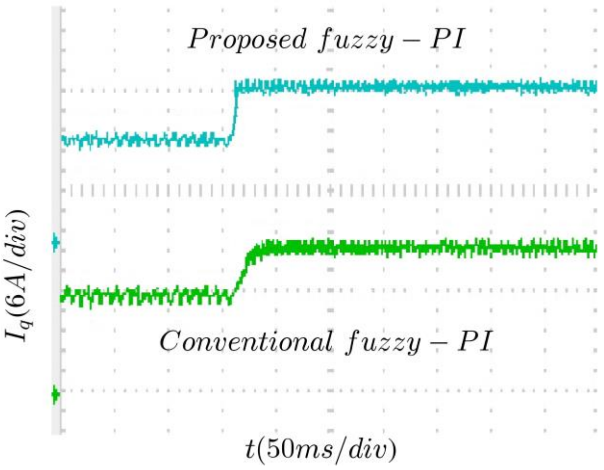

Fig. 16: during suddenly changes.

PI controller is replaced with a new fuzzy-PI. A new model reference adaptive method of fuzzy-PI speed controller is established to improve the dynamic performance of the system.

The equations for estimating the position and the rotational speed are derived and a model is constructed. The simulation and experimental results show that the new fuzzy PI model reference adaptive method can quickly and accurately track the motor position changes. The optimized fuzzy PI speed regulator has small overshoot, small torque ripple and strong robustness compared with the traditional fuzzy PI regulator.

8. References

[1] M. Hannan, M.M. Hoque, A. Mohamed, A. Ayob, Review of energy storage systems for electric vehicle applications: Issues and challenges, Renewable and Sustainable Energy Reviews, 69 (2017) 771-789.

[2] C. Bae, J. Kim, Alternative fuels for internal combustion engines, Proceedings of the Combustion Institute, 36(3) (2017) 3389-3413.

[3] A.M. Andwari, A. Pesiridis, S. Rajoo, R. Martinez-Botas, V. Esfahanian, A review of Battery Electric Vehicle technology and readiness levels, Renewable and Sustainable Energy Reviews, 78 (2017) 414-430.

[4] W. Li, R. Long, H. Chen, J. Geng, A review of factors influencing consumer intentions to adopt battery electric vehicles, Renewable and Sustainable Energy Reviews, 78 (2017) 318-328.

[5] A. Sarigiannidis, M. Beniakar, P. Kakosimos, A. Kladas, Performance evaluation and thermal analysis of interior permanent magnet traction motor over a wide load range, in: 2016 XXII International Conference on Electrical Machines (ICEM), IEEE, 2016, pp. 2662-2668.

[6] [B. Leard, J. Linn, V. McConnell, Fuel prices, new vehicle fuel economy, and implications for attribute-based standards, Journal of the Association of Environmental and Resource Economists, 4(3) (2017) 659-700.

[7] A. Ahmed, A.Q. Al-Amin, A.F. Ambrose, R. Saidur, Hydrogen fuel and transport system: A sustainable and environmental future, International journal of hydrogen energy, 41(3) (2016) 1369-1380.

[8] A. Stephan, B. Battke, M.D. Beuse, J.H. Clausdeinken, T.S. Schmidt, Limiting the public cost of stationary battery deployment by combining applications, Nature Energy, 1(7) (2016) 1-9.

[9] Q. An, J. Liu, Z. Peng, L. Sun, L. Sun, Dual-space vector control of open-end winding permanent magnet synchronous motor drive fed by dual inverter, IEEE Transactions on Power Electronics, 31(12) (2016) 8329-8342.

[10] S. Hirosawa, M. Nishino, S. Miyashita, Perspectives for high-performance permanent magnets: applications, coercivity, and new materials, Advances in Natural Sciences: Nanoscience and Nanotechnology, 8(1) (2017) 013002.

[11] M. Linke, R. Kennel, J. Holtz, Sensorless speed and position control of synchronous machines using alternating carrier injection, in: IEEE International Electric Machines and Drives Conference, 2003. IEMDC'03., IEEE, 2003, pp. 1211-1217.

[12] Z.C.W.Q.W. Shujie, L. Xinran, Data processing system of 21 bit photoelectric encoder [J], Journal of Electronic Measurement and Instrument, 6 (2010).

[13] C. Li, W. Yin, X. Feng, Y. Zhang, Brushless DC motor stepless speed regulation system based on fuzzy adaptive PI controller, Journal of Mechanical & Electrical Engineering, 29 (2012) 49-52.

[14] L. Yong-hua, P. You-guo, Research of the Initial Rotor Position Based on the Principle of Magnetic Orientation [J], Electric Drive, 3 (2010).

[15] S. Maiti, C. Chakraborty, S. Sengupta, Simulation studies on model reference adaptive controller based speed estimation technique for the vector controlled permanent magnet synchronous motor drive, Simulation Modelling Practice and Theory, 17(4) (2009) 585-596.

[16] E. Babaei, M.B. Sharifian, R.A. Farshbaf, S. Hosseini, Verification of a new method for PI block design of MRAS-based sensorless speed estimators, in: 2011 International Conference on Electrical Machines and Systems, IEEE, 2011, pp. 1-6.

[17] A. Khlaief, M. Boussak, A. Chaari, A MRAS-based stator resistance and speed estimation for sensorless vector controlled IPMSM drive, Electric Power Systems Research, 108 (2014) 1-15.

[18] M. Comanescu, L. Xu, Sliding-mode MRAS speed estimators for sensorless vector control of induction machine, IEEE Transactions on Industrial Electronics, 53(1) (2006) 146-153.

[19] H.M. Kojabadi, L. Chang, R. Doraiswami, A MRAS-based adaptive pseudoreduced-order flux observer for sensorless induction motor

drives, IEEE Transactions on Power Electronics, 20(4) (2005) 930-938.
[20] T. Orlowska-Kowalska, M. Dybkowski, Stator-current-based MRAS estimator for a wide range speed-sensorless induction-motor drive, IEEE Transactions on industrial electronics, 57(4) (2009) 1296-1308.
[21] J. Zhao, M. Lin, D. Xu, L. Hao, W. Zhang, Vector control of a hybrid axial field flux-switching permanent magnet machine based on particle swarm optimization, IEEE Transactions on Magnetics, 51(11) (2015) 1-4.
[22] J.R. Fard, M. Ardebili, Design and control of a novel yokeless axial flux-switching permanent-magnet motor, IEEE Transactions on Energy Conversion, 34(2) (2018) 631-642.

HOW TO CITE THIS ARTICLE

H. Radmanesh, J. Rahmani Fard, Hybrid Fuzzy Algorithm for the Novel Yokeless Axial Flux-Switching Permanent-Magnet Motor, AUT J. Elec. Eng., 52(2) (2020) 169-178.

DOI: 10.22060/eej.2020.18045.5342